Axisymmetric Stagnation-Flow Freezing of Saturated Air Vapor

Shokrgozar Abbasi, Ali*+; Niouki, Mohammad Javad

Department of mechanical engineering, Payame Noor University, Tehran, I.R. IRAN

ABSTRACT: *Stagnation flow freezing of saturated air vapor in axisymmetric cylindrical coordinates system is considered. It covers a detailed discussion on how the ice layer and the ongoing phenomenon changes with time. The fluid along z-direction, with strain rate a impinges perpendicularly on a substrate flat plate and because of the lower plate temperature than the freezing temperature of water, condensation is occurred, then water probably starts to freeze. The flow is assumed laminar with constant properties and that the density changes with temperature can be negligible. The momentum equations are converted to an ordinary differential equation by use of appropriate similarity transformations. The obtained ordinary differential equation is solved by using fourth order Rung_Kutta Method. Two methods have been used to solve the energy equation: finite-difference numerical techniques and similarity solutions. The results of energy equations of these two methods are compared together for validation. Based on the obtained results, substrate plate temperature for initiation of water vapor freezing is reduced by reduction of far field saturated air temperature. Interestingly, freezing start time increases with increasing of far field saturated air temperature first and then reduces rapidly as the increasing of the far field temperature is continued. The ultimate thickness of the ice is also presented. One of the most important achievements of this paper is determining the final thickness of ice in an analytical manner using only the air temperature profile, which can be used as a reliable method to validate the numerical solution*.

KEYWORDS: *Water vapor freezing, Stagnation flow, Unsteady flow, Viscous fluid, Incompressible flow, Similarity solution, Ice thickness.*

INTRODUCTION

Solidification is one of the most interesting phenomena in natural processes and industrial applications which can comprise heat transfer accompanied by phase change. In the present study, freezing of saturated air vapor in the axisymmetric stagnation flow is investigated. Glass, metal, plastic and oil industries, providing food and other corresponding industries needs a good insight of solidification behavior as the nature of solid growth. Furthermore, studies of phase change in stagnant media, better understanding of convection effect upon the interface behavior and solidification properties are needed by industrial demand such as the desire for more homogenous semi-conductor crystals, in nuclear industry, as well as the better understanding of natural ice formation.

**To whom correspondence should be addressed.*

+ E-mail: shokrgozar.ali@pnu.ac.ir

1021-9986/2023/12/4272-4283 12/$/6.02

Especially, in the aerospace industry, freezing of saturated air vapor and the conditions for its freezing in front of the aircraft is of great significance. This phenomenon may also occur at the tip of a missile. Investigations in the field of heat transfer in phase change or freezing in stagnation flow and related studies are as follows.

The classic problem of ice formation in polar seas was solved using the analytical method by Stefan [1]. A one-dimensional heat flux for phase change issues was presented by Goodrich [2]. An experimental study for natural convection in the fluid border between liquid and solid phases was investigated by *Sparrow and et a*l. [3]. Numerical methods for solving problems of freezing the flow of natural convection between two isolated plates were presented by Lacroix [4]. Three-dimensional numerical study for free convection with phase change in a channel with rectangular a cross-section was considered by *Yeoh et al*. [5]. An analysis about combining hydrodynamic behavior with behavior of the solid-liquid boundary layer of fluids, which is located between two freezing isolated plates, was investigated by Hadji and Schell [6]. A method for calculating time-dependent heat flux caused by natural convection during freezing fluid between two isolated plates was presented by Hanumanth [7]. Providing an integrated model for continuous phase change issues was investigated by *Curtic et al*. [8]. The problem of freezing molten liquid drops on a rigid plate model was solved by *Trapaga et al* [9] and comparison between numerical modeling and laboratory results of deformation and freezing of a drop on a cold plate is conducted by *Watanabe et al* [10]. Evaluation of an existing model transformation and freezing adjusted to a drop impinging on the substrate plate is also presented by *Marchi et al* [11]. The flow of heat transfer of viscous fluid produced by the axisymmetric stagnation flow on a flat plate that at its coordinates has damped oscillatory motion was investigated by Weidman and Mahalingam [12]. Investigation of flow and heat transfer in asymmetric three-dimensional viscous stagnation flow was presented by Shokrgozar and Rahimi [13]. Viscous stagnation flow and heat transfer in asymmetric three-dimensional system with suction and blowing was considered by Shokrgozar and Rahimi [14]. The exact solution of the unsteady two-dimensional stagnation flow and heat transfer on a heated plate was presented by Shokrgozar and Rahimi [15]. The two-dimensional stagnation flow and heat transfer on an accelerated flat plate was investigated by Shokrgozar and Rahimi [16]. Axisymmetric stagnation flow and heat transfer on an accelerated flat plate was presented by Shokrgozar et al [17]. Stagnation flow solidification of an inviscid fluid that freezes at the common border was considered by Brattkus and Davis [18]. The problem of Stephen solidification for viscous fluid in stagnation flow was solved by Rangel and Bian [19]. Freezing of viscous liquid stagnation point was investigated in the two-dimensional Cartesian coordinate system by Bian and Rangel [20], however, this problem also considered by Shokrgozar and Rahimi [21]. In the recent paper, it has been shown numerically and analytically that the results of [20] are not correct. Freezing of incompressible fluid in unsteady axisymmetric stagnation flow has also been investigated by Shokrgozar [22].

In some cases, it is necessary to prevent freezing of water vapor to prevent destruction. An example of it occurs in the freezing of water or water vapor in the soil, which will be examined due to the latest results of. *Zhao et al*. [23] who have conducted a series of one-side freezing experiments to evaluate the effect of fine grain content and initial water content on moisture and frost susceptibility of the coarse-grained soil. In these experiments, coarse-grained soil with different contents of clay in an open system with water supply without pressure was desired. Their experimental results show that by simulating the impervious cover, a thin ice layer appears at the cold end boundary, which is an important reason for the increase in freezing of coarse-grained soil. The effect of external water on the freezing of coarse-grained soil cannot be ignored, and with the increase of fine-grained soil, the amount of external water increases.

Zhang et al. [24] conducted a series of experiments for different freezing modes during freezing and thawing to study the behavior of water-heat-steam in coarse-grained soil under high-speed railway in cold regions with free water. Fluorescein has been used as a tracer for elevation and liquid water changes in external water sources. When the soil sample freezes, the external water migrates into the soil and when it thaws, the internal water of the soil sample migrates out. The amount of water used affects the penetration of frost during freezing and thawing. Increasing the freezing steps leads to a more uniform distribution of water

content. Moisture migration in high-speed rail bed occurs mainly by vapor migration during long cold winters and winters with slow temperature drop.

In cold regions, freezing and thawing cycles play an important role in many engineering and agricultural applications and make the studies of water flow and heat transfer in soil much more complicated due to phase changes. *Zheng et al*. [25] developed a fully coupled numerical module to simulate the simultaneous movement of water, steam and heat during freeze-thaw cycles and incorporated it into the Hydrus-1D software in clod regions. They concluded that the isothermal fluid flux is the most important component of the total flow in most of the soil depth except for the frozen layer, which is normally reduced by 1 to 5 orders of magnitude before freezing. Instead, thermal vapor flux is the dominant moisture transport mechanism in the frozen layer and contributes about 10% to ice formation. *Liu et al*. [26] investigated the damage to airport runways and highways in water vapor freezing, which causes frost damage and destruction. They concluded that the unfrozen water content decreases with temperature when the water content is higher. At higher water contents or lower (cooler) temperatures, water migration in the soil column is more significant. Under a given temperature gradient, the lower the freezing point, the lower the depth of freezing, the smaller the migration of liquid water, finally the smaller the volume fraction of ice. Freezing of air vapor in Cartesian two-dimensional stagnation flow has also been investigated by Shokrgozar and Ghayeni [27]. *Zahmatkesh et al*. [28] are investigated the entropy generation in the stagnation flow of nanofluid on a cylinder with transpiration using similarity solution. The results of the research show that with the increase in nanoparticle fraction, the heat transfer coefficient increases, at the same time, the radial and axial components of the wall shear stress increase. Furthermore, the inverse estimation method can also be called among the stagnation flow solving methods. *Montazeri et al*. [29, 30] presented a code based on the Levenberg–Marquardt method, which is used to the reverse heat transfer of an axisymmetric stagnation flow on a cylinder with uniform transpiration. This technique is based on an iterative method that must minimize the sum of the least squares of the error values between the estimated and measured temperatures. The optimal coefficient of sensitivity of heat flux estimation has been calculated and based on the results, it is emphasized that suction increases the accuracy of calculations and vice versa, blowing decreases the accuracy. However, the axisymmetric freezing of water vapor in saturated air, which has differences not only in the type of coordinate system but also in the objectives, has not been investigated so far.

In this manuscript, the water vapor freezing in the axisymmetric stagnation flow is studied. The manuscript has a detailed debate on how the ice layer and the ongoing phenomenon changes with time. The fluid flow is assumed incompressible, viscous and in laminar regime with constant properties. The Magnus forces due to their rotation in response to shear are assumed negligible in the present study. In addition, the effects of mass diffusion, here are neglected as well, for simplicity. Due to the fluid deal with the temperature lower than the freezing temperature of water, the vapor becomes liquid and then, if the substrate temperature is below enough, ice will be produced. In such cases ice is built not as a 100% solid. It is porous (frost) and its density increases with time. Here, if high heat transfer rate and enough time to settle at the lowest node do not exist distilled water may be flowing into frost. This article assumes that there is adequate time to settle fluid only at the nearest cells to ice so the frost production assumption is excluded thrush and it requires a separate investigation.

PROBLEM FORMULATION

Take the tip of a missile for example. In Fig. 1a, axisymmetric coordinates with corresponding (u, w) velocities respect to (x,z) is shown Saturated air stagnation flow with $a(t)$ strain in the z direction approaches perpendicular to the plate at $z = 0$. Properties of air, vapor and water are assumed constant. If the temperature of the lower plate is low enough, wate vapor in the air will begin to freeze. Because the desired stagnation flow, heat transfer is distributed uniformly in the substrate and so the ice surface will be flat. Hence, ice can be considered as an imaginary flat plate at solid-fluid interface is moved towards fluid as $S(t)$distance in each time step with variable velocity and acceleration, $\dot{S}(t)$ and $\ddot{S}(t)$ respectively. Also, in Fig. 1b, the temperature distribution in the stagnation flow is shown schematically.

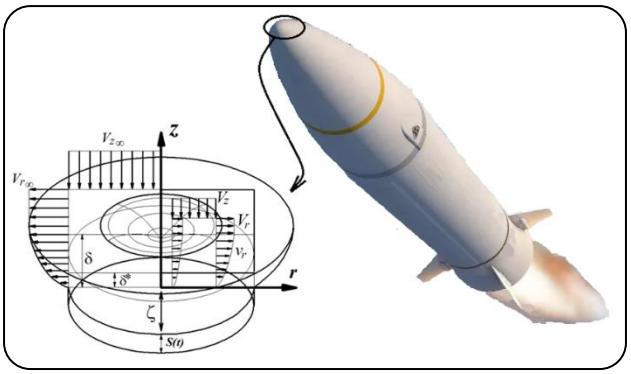

Fig. (1a): Viscous layer (An example of application)

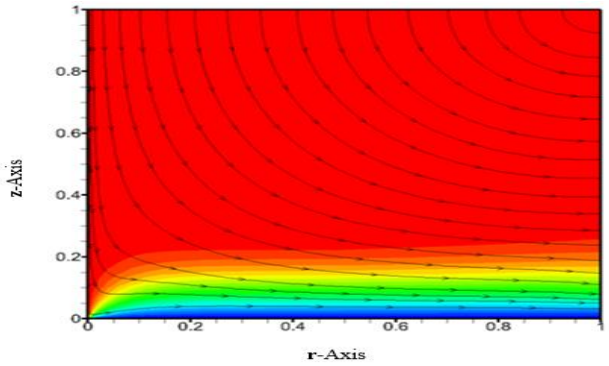

Fig. (1b): Temperature (Schematic of the problem)

Note, the ice thickness will be constant throughout the flat plate because of the uniform heat transfer at the solid-liquid interface, so the solid-liquid interface is assumed as imaginary plate. Refer [17] for more explanation over imaginary plate instead of solid-liquid interface. Due to temperature changes in the air, densities of vapor and air are changed as well. These changes will be negligible, as the flow is assumed incompressible. However the volume change of vapor to water that has affection in the cell size is taking into account. In this case, vapor and tiny particles of water exist together, but the water particles will only have the opportunity to settle at the lowest cell's row as the lowest velocity and the highest water weight exists in this row. Otherwise, it may happen that tiny water particles have the opportunity to settle at all cells rows and frost is produced in this mode, which is outside the scope of this article. Note that the Magnus forces due to their rotation in response to shear are assumed negligible. The effects of mass diffusion are also neglected for simplicity. Mass and Navier–Stokes equations for Newtonian, laminar, incompressible, unsteady state with constant density and viscosity properties fluid read:

Mass:

$$\frac{\partial v_r}{\partial r}+\frac{v_r}{r}+\frac{\partial v_z}{\partial z}=0 \tag{1}$$

Momentum:

$$\frac{\partial v_r}{\partial t}+v_r\frac{\partial v_r}{\partial r}+v_z\frac{\partial v_r}{\partial z} = -\frac{1}{\rho}\frac{\partial p}{\partial r} + \nu\left(\frac{\partial^2 v_r}{\partial r^2}+\frac{1}{r}\frac{\partial v_r}{\partial r}-\frac{v_r}{r^2}+\frac{\partial^2 v_r}{\partial z^2}\right) \tag{2}$$

$$\frac{\partial v_z}{\partial t}+v_r\frac{\partial v_z}{\partial r}+v_z\frac{\partial v_z}{\partial z} = -\frac{1}{\rho}\frac{\partial p}{\partial z}+\nu\left(\frac{\partial^2 v_z}{\partial r^2}+\frac{1}{r}\frac{\partial v_z}{\partial r}+\frac{\partial^2 v_z}{\partial z^2}\right) \tag{3}$$

Unsteady energy equation in fluid region (dissipation and radiation heat transfer are neglected) reads[27]:

$$\frac{\partial T}{\partial t}+v_r\frac{\partial T}{\partial r}+v_z\frac{\partial T}{\partial z} = \alpha\left(\frac{\partial^2 T}{\partial r^2}+\frac{1}{r}\frac{\partial T}{\partial r}+\frac{\partial^2 T}{\partial z^2}\right) + \frac{\partial m_{vl}}{\partial t}\frac{H_{vl}}{\sum_{j=1}^{3} m_i C_i} \tag{4}$$

Notice conductivity and heat capacity coefficient are constant (k and C respectively) also $du \approx cdT$ is assumed where p, ρ, ν and α are the fluid pressure, density, kinematic viscosity, and thermal diffusivity.

Energy equation in solid phase (ice) reads[27]:

$$mC\frac{\partial T}{\partial t} = k\frac{\partial T}{\partial N}A_N - k\frac{\partial T}{\partial S}A_S \tag{5}$$

And the energy equation (boundary condition) at interface before reaching freezing temperature becomes:

$$\sum_{j=1}^{3}\rho_i c_i \forall_i \frac{\partial T}{\partial t} = kA_N\frac{\partial T}{\partial N} - kA_S\frac{\partial T}{\partial S} + \left(\frac{m_v^n - m_v^{n+1}}{\Delta t}\right)H_{vl} \tag{6}$$

where the left term in the equation is energy moving boundary and right terms are conductive heat transfers and heat source from left to right, respectively. Also, the energy equation (boundary condition) at interface after reaching freezing temperature becomes:

$$\rho_l h_{ls} A_{N,S}\frac{\partial S}{\partial t} = kA_N\frac{\partial T}{\partial N} - kA_S\frac{\partial T}{\partial S} \tag{7}$$

That the left term is the source and the right terms are conductive heat transfers from up and down, respectively.

Also, by using curve fitting, the relative humidity from psychometric chart can be defined as:

$$\omega_{i,k}^{n+1} = b_1 + b_2 T_{i,k}^{n+1} + b_3 \left(T_{i,k}^{n+1}\right)^2 + b_4 \left(T_{i,k}^{n+1}\right)^3 + b_5 \left(T_{i,k}^{n+1}\right)^4 \quad (8)$$

That can be used for a range of 0 to 70 degrees Celsius and after linearizing by Newton-Raphson method reads,

$$\omega_{i,k}^{n+1} = \omega_{i,k}^{n} + \left(b_2 + b_3 2T_{i,k}^{n} + 3b_4 \left(T_{i,k}^{n}\right)^2 + 4b_5 \left(T_{i,k}^{n}\right)^3\right)\left(T_{i,k}^{n+1} - T_{i,k}^{n}\right) \quad (9)$$

In which Subscripts (i,k) are node numbers in r and z directions, respectively, Superscript $(n+1)$ is present time, $\omega_{i,k}^{n+1}$ is the relative humidity for present temperature and $b(1/°C)$ coefficients are:

b_1=3.744E-03, b_2=2.820E-04, b_3=7.360E-06, b_4=2.200E-07, b_5=3.270E-09

As $m_v = \omega_{i,k} m_{air}$, the equation (9) is obtained for linearizing the numerical solution of the energy equation.

SIMILARITY SOLUTION

Fluid flow solution

According to Ref. [17] and integrating equations (1) to (3) outside boundary layer, the classical equations of potential flow solution is as follows:

$$V_r = a(t)r \quad (10)$$

Note, boundary layer is defined here as the edge of the points where their velocity is 99% of their corresponding potential velocity. By inserting (10) in continuity equation (1) and after integrating:

$$V_z = -2a(t)\ \zeta \quad (11)$$

Where $\zeta = z - S(t)$ and $S(t)$ is the amount of plate displacement in z- direction and is assumed to be positive when the plate moves toward the impinging flow. Hence, $S(t)$ and, then, ζ are functions of time. These recent equations (10-11) are the boundary condition equations in viscous layer. A reduction of the Navier-Stokes equations is sought by the following coordinate separation in which the solution of the viscous problem inside the boundary layer is obtained by composing the inviscid and viscous parts of the velocity components, Ref [17]:

$$u = a(t)rf'(\eta) \quad (12)$$

$$w = -2\sqrt{\nu/a_0}\ a(t)f(\eta) \quad (13)$$

$$\eta = \sqrt{\nu/a_0}\ \zeta \quad (14)$$

Where terms involving $f(\eta)$ in (12), (13) comprise the similarity form for unsteady stagnation flow and prime denotes differentiation with respect to η. Moreover, a_0 is the reference potential flow strain rate at the time =0. By insertion of transformations (12)-(14) into (2) - (3) yields an ordinary differential equation in terms of $f(\eta)$:

$$f''' + f''\left(\tilde{S} + 2\tilde{a}f\right) + \left(-\tilde{a}f' - \frac{1}{\tilde{a}}\frac{d\tilde{a}}{d\tau}\right)f' - \frac{1}{\tilde{a}}\frac{d\tilde{p}}{d\xi} = 0 \quad (15)$$

, where $-\frac{1}{\tilde{a}}\frac{d\tilde{p}}{d\xi} = \frac{1}{\tilde{a}}\frac{d\tilde{a}}{d\tau} + \tilde{a}$

With Boundary conditions:

$$\eta = 0 : \ f = 0, f' = 0$$
$$\eta \to \infty : \ f' = 1 \quad (16)$$

The ODE (15) is solved numerically using a shooting method trail and error based on Runge-Kutta algorithm.

Heat transfer solution

Dimensionless temperature defined as:

$$\theta = \frac{T(\eta) - T_\infty}{T_w - T_\infty} \quad (17)$$

Making use of transformations (12) - (14), equation (4) may be written as:

$$\theta'' + \Pr.\theta'[2f + \tilde{S} + \tilde{\dot{S}}_{vl}\,.\,Evap] = 0 \quad (18)$$

Where,

$$Evap = -\frac{\dot{m}_{air}\,H_{vl}}{\sum_{i=1}^{3} m_i c_i}(b_2 + 2b_3\theta + 3b_4\theta^2 + 4b_5\theta^3) \quad (19)$$

Here, $\tilde{\dot{S}}_{vl}$ dimensionless water vapor condensing velocity is defined as:

$$\tilde{\dot{S}}_{lv} = \tilde{\dot{S}} \times \frac{\rho_{Water}}{\rho_{Vapor}} \quad (20)$$

With boundary conditions as:

$$\eta = 0 : \theta = 1$$
$$\eta \to \infty : \theta = 0 \quad (21)$$

Where θ is dimensionless temperature, the subscript w and ∞ refer to the conditions at the wall and in the free stream, respectively, $Pr = \frac{\nu}{\alpha}$ is Prandtl number and prime indicates differentiation with respect to η.

NUMERICAL SOLUTIONS OF HEAT TRANSFER EQUATIONS

The heat transfer similarity solution is a quasi-steady solution of the heat transfer equation and for all the times do not provide temperature profiles. However, it is used to evaluate the numerical solution. By entering the obtained velocities from momentum equations into the energy equation, it is linearized and ADI(Alternative Direction Implicit) and TDMA(Three Diagonal Matrix Algorithm) are used as solution methods. The energy equation at the interface before water reaches its freezing point (6) consists of water and vapor, which these values should be determined by relative humidity. However, the relationship between relative humidity and temperature (8) is strongly nonlinear. Newton-Raphson's method for linearization is used (9). The energy required for changing the cell temperature comparing to condensing enthalpy is many order of times less. So a big under relaxation factor is necessary for solidifying latent enthalpy term in energy equation to balance the temperature between cells not diverge from losing and answer. In this statue, trial and error is required to solve the problem together with very small steps at the same time the solution is implicit. When fluid temperature reaches the freezing point as the temperature of the interface remains constant, upstream temperature changes are stopped and the dominant energy equation in interface is (7) that is the same equation will be freezing at the boundary. The resolution of the process in numerical solution of heat transfer is as follows:

1. Very little time step in the field of fluid by ADI method and the use of TDMA with a relaxation factor will be resolved.
2. Solved by trial and error will be corrected, then slightly reduced relaxation factor to finally be eliminated.
3. The energy equation can be solved at the interface as follows:

3.1 If the temperature has not yet reached the water freezing point, just changed the cell interface temperature and the above steps are repeated again.

3.2 If the temperature reaches the water freezing point temperature the interface temperature have not changed and only the latent enthalpy heat of cells water to turn into ice are provided.

4. If the interface freezing temperature in the first row equals the maximum temperature upon freezing, stop freezing.
5. If the interface freezing temperature in the first row is less than the maximum temperature upon freezing, due to a thin layer of ice, some of the previous temperature gets closer to zero and the process is repeated from the beginning.
6. Freezing velocity $(\dot{S})$ is entered into the momentum equation (15) for solving using the fourth order rung-kutta method.

The above steps are continued until fluid temperature in the interface reaches the freezing point. Since the variation in the size of the mesh from 0.2 to 0.1mm result a negligible variation in the T_{sub} (Fig. 7), 0.2mm cell size is selected in this paper**.**

VALIDATION

Exact solution is used for solving the momentum equations, so there no additional requirement for validation. In order to validate the obtained heat transfer results, the exact solution of the energy equation is used. The answers of the exact solution are useful only for times just before the steady state condition. In this section, numerical and exact solutions of energy equations are compared together for the four different quantities of far field air temperatures, 1, 15, 25, and 40℃, respectively. The results in Figs. 2a_2d show that there are a maximum error of about 3%, and a Minimum error of about 0% between the exact solution and the numerical solution. Contrary to the numerical solution, considering that in the performed exact solution, the volume change of the cells due to water distillation is not yet taken into account, hence, the magnitude of error is negligible. Therefore, there are good matches for these diagrams quantities. In addition, the reason for change in the error rate variations is the increasing amount of water present at higher air temperatures, which causes a higher change in the volume of the cells. Fortunately, the freezing calculations are based on the numerical solution of the energy equation and

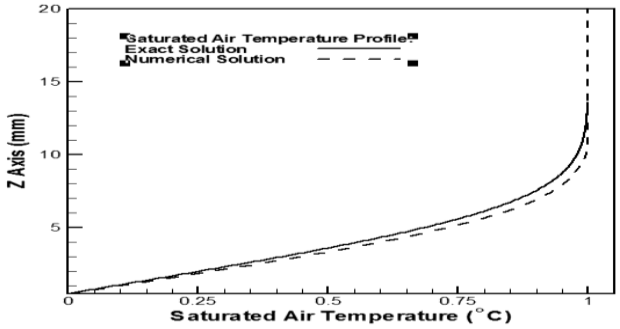

Fig. (2a): Comparing the numerical and exact solutions of energy equation ($Tair_{\infty} = 1$℃, Max. $err = \%3$)

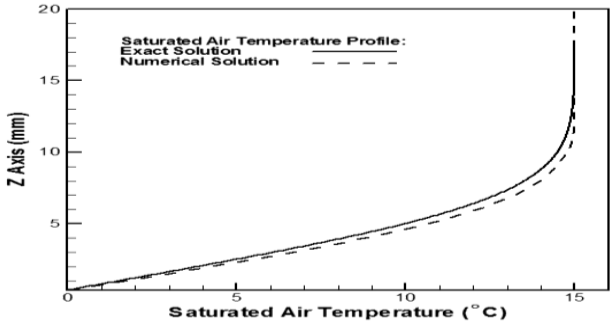

Fig. (2b): Comparing the numerical and exact solutions of energy equation ($Tair_{\infty} = 15$℃, Max. $err = \%2.5$)

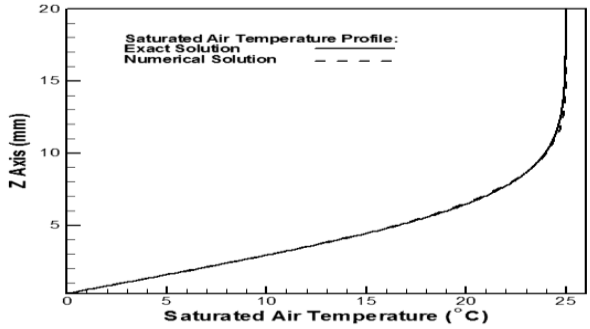

Fig. (2c): Comparing the numerical and exact solutions of energy equation ($Tair_{\infty} = 25$℃, $Max.\ err \approx \%0$)

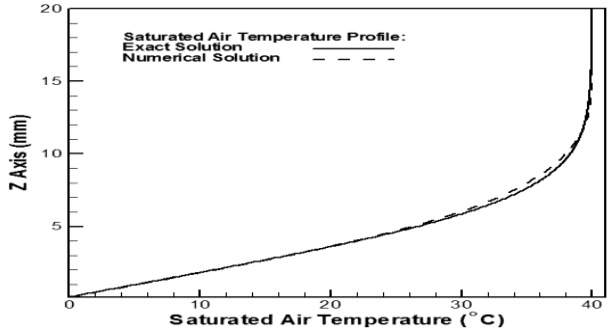

Fig. (2d): Comparing the numerical and exact solutions of energy equation ($Tair_{\infty} = 40$℃, $Max.\ err = \%0.5$)

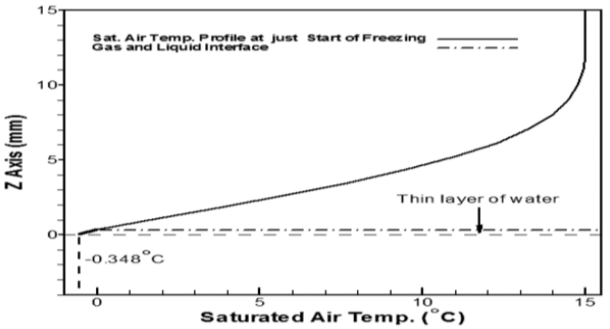

Fig. (3): Saturated Air Temperature 15º C , Substrate Plate Temperature -0.348 ° C

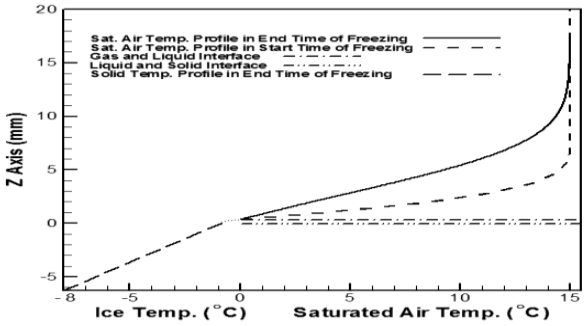

Fig. (4): Saturated Air Temperature 15º C , Substrate Plate Temperature -8º C

the exact solution is used only for validation. Another reason for the small differences between the values of numerical and exact solution can be caused by linearization in the numerical solution in relative humidity term.

PRESENTATION OF RESULTS

To begin with, let us start with the following conditions**.** We assume the saturated air with a temperature of 15 °C impinges on a cold substrate plate at -0.348 °C. The problem solution in this case is shown in Fig. 3. As can be seen, under this condition, only a thin layer of water is formed at 0 °C while ice is still absent. In fact, this boundary temperature is the temperature at which water begins to form**,** which, further temperature drop of the substrate plate will result in formation of ice. Note that this temperature is achieved by trial and error.

In the next step, we lower the substrate plate temperature further. For example, the substrate plate temperature is -8.0 °C. As shown in Fig. 4, the thickness of the ice reaches about 6.25 mm and then stabilizes. After freezing stops, a thin layer of 0.0° C water is formed again, but does not freeze.

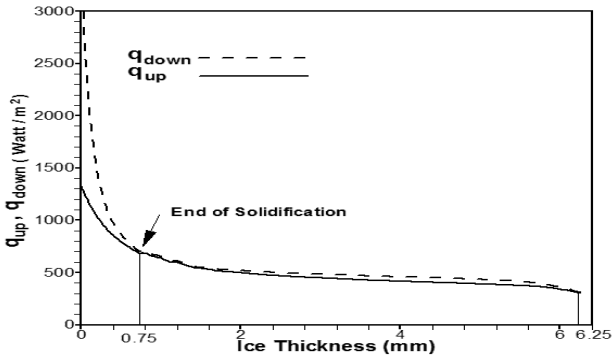

Fig. (5): Saturated Air Temperature 15 ℃, Substrate Plate Temperature -8 ℃
Qup is heat transfer from cells of the first row of the saturated air region to the second row
Qdown is heat transfer from the cells of the first row of the ice region to the first row of the saturated air region

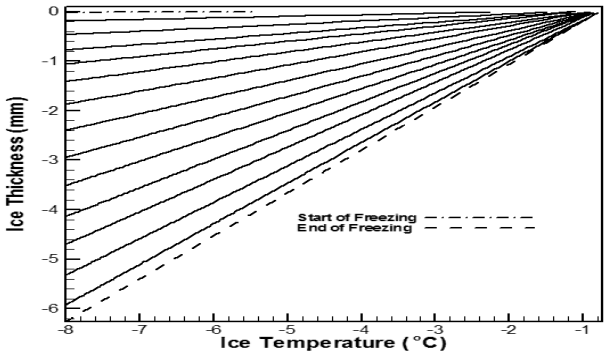

Fig. (6): Evolution of the ice temperature profile (Saturated Air Temperature 15º C , Substrate Plate Temperatures -8º C)

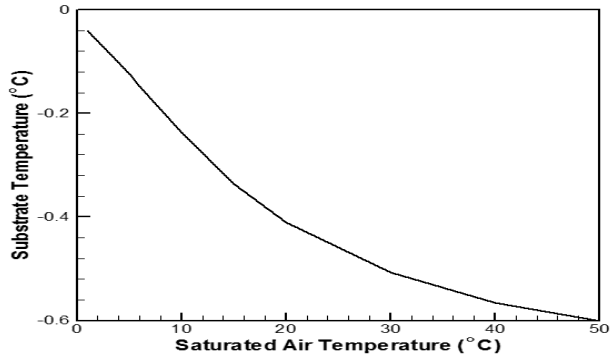

Fig. (7): Substrate Plate Temperatures for Start Freezing in Different Saturated Air Temperature (1 to 55)

As seen in Fig. 5, freezing is continued to a thickness of 6.25 mm. However, when ice thickness reaches 0.75 mm (the point indicated in the diagram), the difference in the heat input to the first row in the saturated air region and its output is very small at about 9 watt/m2. This means that

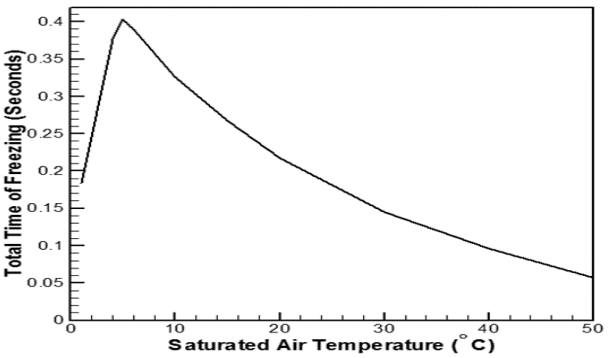

Fig. (8): Total time required to start ice formation versus Different Saturated Air Temperature (1 to 55), N=75, cell size = 0.2 mm

the input heat of the cells in the first row is very close to the output heat of those cells and is insufficient for freezing the vapor. In these conditions, it seems that freezing will practically stop.

In Fig. 6, evolution of the ice temperature profile is shown. As shown in this Fig., the ice temperature slope is steadily changing to reach the ice-free stop point. However, for any given temperature, this slope will be a certain amount. The temperature slope of ice constantly changes until reaching the stable state of equilibrium conditions. Note that this process will be the same for different air temperatures, and the temperature of 15 ℃ is chosen as a sample.

The substrate plate temperatures for initiation of freezing are also calculated for different saturated air temperatures. The results can be seen in Fig. 7. This Fig. shows one of the most important results in this paper. For example, for far field air temperature $Tair_{\infty} = 5℃$, the maximum substrate temperature should be lower than $T_{sub,max} = -0.14$ ℃ to start freezing, and for far field air temperature $Tair_{\infty} = 20℃$, substrate temperature should be lower than $T_{sub,max} = -0.42℃$. As we expected, substrate temperature closes to zero degree as decreasing the far field temperature. Notice, since the variation in the size of the mesh from 0.2 to 0.1mm result a negligible variation in the $T_{sub,max}$ (Fig. 7), it can be concluded that the mesh size of 0.2mm produces relatively accurate results.

In Fig. 8, the total time required for ice formation versus change in saturated air temperature is presented as well. So a cell size (0.02 mm) is selected in order to demonstrate the trend of changes in the freezing start time versus far-field air temperature. In fact, in this Fig., the consequence of approximating the condensation-freezing

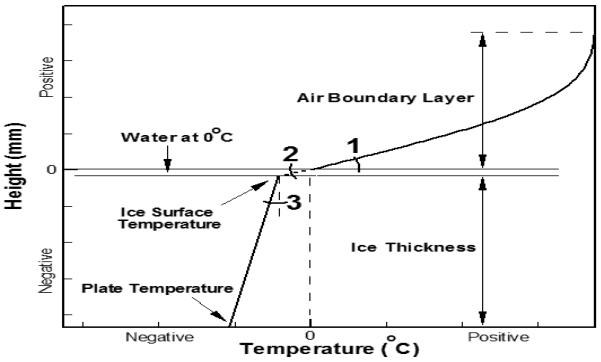

Fig. (9): Schematic temperature profiles of ice and air

location as in the center of the computational cell next to the substrate-ice solid surface is shown. Interestingly, at first, time versus air temperature increases with a sharp slope and then drops (about 5o C) with a nearly same slope, and subsequently temperature drop decreases at temperatures above 20 ℃,. But one might ask; why? Time condensation and freezing water vapor in the air is a function of two variables, far field air temperature, and water vapor content in the air. Of course, one cannot expect that these two phenomena are linear as the relative humidity in the air is not linear. So far, close to zero degrees Celsius temperature vapor and consequently the amount of water available to freeze severely reduced. Therefore, the time required for condensation and freezing the dart towards zero. In other words, in the start-up transient, the thickness of the thermal viscous layer increases as the square root of elapsed time as:

$$\delta \approx K\sqrt{t} \tag{22}$$

where δ is thermal viscous layer thickness and K is a constant. The Eq. (22) can be obtained by the scaling analysis in energy equation. The temperature T profile in the boundary layer is simply represented as,

$$\frac{T_\infty - T_{\text{sub}}}{T - T_{\text{sub}}} \approx \frac{y}{\delta} \tag{23}$$

where the y value of interest can be taken as a fraction,, $1/N$, of the thermal viscous layer thickness witch N is number of cells; by setting $y = \frac{\delta_{ss}}{N}$ (δ_{ss} is the steady state viscous layer) then elapsed time reads:

$$\text{t} \approx \left(\frac{\delta_{ss}}{NK}\right)^2 \left(\frac{T - T_{\text{sub}}}{T_\infty - T_{\text{sub}}}\right)^2 \tag{24}$$

Note that in a physical experiment, condensation should immediately begin at the substrate surface, however in numerical calculations, the size of the nearest cell to the substrate controls the time at which condensation begins because the low temperature imposed by the substrate reaches the center of that cell by diffusion. So the time to beginning of condensation should vary as the inverse square of cell number, N, according to Eq. (24).

In this section, we attempt to find a simple and clever way to determine the final thickness of the ice. We want to obtain the final thickness of ice by only the air temperature profile, without any further steps to solving the problem completely. It worths noticing that solving this problem could be very complicated and time-consuming. In addition, doing so will confirm the numerical solution to the problem solving in the ice formation. Note that we have already evaluated the obtained temperature profiles by exact solution of the heat transfer equation in the fluid region. Here, we evaluate the final thickness of ice using an analytical solution as well. The schematic diagram of temperature profiles under equilibrium conditions is shown in Fig. 9. First, we must find the temperature profile of saturated air at the substrate plate temperature at which freezing stops. The slope of this temperature profile at the freezing point, angle 1 in Fig. 9, can be easily calculated. Note that angle 2 is related to angle 1 with the following relation:

$$\frac{\Delta T_1}{R_{tot1}} = \frac{\Delta T_2}{R_{tot2}} \tag{25}$$

where ΔT_1 is the temperature difference of the first and second rows of the cells at the air, ΔT_2 is the temperature difference of the first row of cells at the air and the first row of cells at the ice, R_{tot1} and R_{tot2} are the total thermal resistance between the corresponding rows, respectively. The later equation is used to determine ΔT_2 without solving the problem completely. Finding ΔT_2 is very important and this relation is the golden key of this analytical method, which simplifies calculation of ice thickness as follows:

$$\Delta z_{Tot} = -k_{Ice}.\Delta T_3 / q_{Down} \tag{26}$$

which ΔT_3 is the temperature difference between the substrate plate and the temperature in equilibrium conditions of the first row of cells at the icing phase. These calculations are performed for Fig. 4 and it can be seen that they closely match the numerical calculations.

CONCLUSIONS

In this article, freezing of water in saturated air stagnation axisymmetric flow is investigated on a flat plate. The air with a relative humidity of 100% impinges on a cold plate and is frozen after distillation. For freezing, however, the temperature of the substrate plate should be sufficiently cold. Momentum equations have been solved using the similarity solution method. The solution approaches of the energy equation have also been divided into two sub-sections: Numerical and exact solutions for energy equation in three phases consist of gas, liquid, solid and solid-liquid interface are used and these equations are solved at any step simultaneously. According to the results, by increasing the far field air temperature ($Tair_\infty$) from 0℃ to 5℃, time for initiation of water vapor freezing is increased and subsequently, by increasing $Tair_\infty$ its time decreases until at more than 50℃. The temperature profiles are represented, as well. The highest temperature of the substrate plate ($T_{sub,max}$) to initiate water vapor freezing in the air are also presented with different temperatures($Tair_\infty$). In addition, results of the thickness of ice formed by freezing at temperatures lower than the freezing initiation temperature ($T_{sub,max}$) are shown, which is the main objective of this article. The most intelligent finding of this article is an easy analytical solution that determines the ultimate thickness of ice with the presence of the air temperature profile. This method can also be used to validate the numerical solution.

Nomenclature

English

$a(t)$	Time-dependent flow strain rate
$\tilde{a}$	Dimensionless Time-dependent strain rate
a_0	Reference potential flow strain rate at the start of time
A	Area
b	Coefficient (1/℃)
C	Heat capacity coefficient
$Evap$	Auxiliary variable
H	Latent enthalpy of water
H_{ls}	333.4 kJ/kg (liquid to solid)
H_{vl}	2501.0 kJ/kg (vapor to liquid)
k	Thermal conductivity
K	Constant
m	Mass of any participants
$\dot{m}$	Mass flow rate
N	Number of cells
p	Pressure
$\tilde{p}$	Dimensionless pressure
Pr	Prandtl number
$S, \dot{S}, \ddot{S}$	Thickness, velocity and acceleration of ice evolution, respectively, in z-direction
$\tilde{S}, \tilde{\dot{S}}$	Dimensionless thickness and velocity of ice evolution, respectively, in z-direction
t	Time
T	Temperature
$Tair$	Temperature of air
$T_{sub,max}$	The temperature of substrate for start of freezing
$\forall$	Volume
u, w	Velocity components near the plate in x, z directions
$\tilde{u}, \tilde{w}$	Dimensionless velocity components near the plate in x, z directions
U, W	Potential region velocity components in x, z directions
x, y,z	Cartesian coordinates

Greek

δ	Viscous layer thickness
δ^*	Displacement viscous layer thickness
ζ	Variable $(z - S(t))$
η	Similarity variable
θ	Dimensionless temperature
ν	Kinematic viscosity
ξ	Dimensionless x-axis
ρ	Density
τ	Dimensionless time
ω	Humidity ratio $= m_{vapor}/m_{air}$

Subscripts

0	At the nearest calls of mesh to the ice (Or first row of cells in fluid region)
∞	Free stream (far-field)
i,k	Node (or Cell) row and column numbers in x and z directions, respectively
j	1 to 3 numbers (air, vapor and water)
l	Liquid phase (Water)
ls	Liquid to solid (Phase change)
max	The maximum substrate temperature that the first row of cells (or nearest cells to ice) can freeze
N	North
S	South

ss	Steady state
sub	Substrate plate
$total$	Total time of freezing the first cells row
vl	Vapor to liquid (Phase change)
v	Vapor

Superscripts

$\sim$	Dimensionless
n	Timing step (old)
$n+1$	Timing step (new)

Received : May.03, 2023 ; Accepted : Jul.10, 2023

REFERENCES

[1] Stefan, J., "About the Theory of Ice Formation, in Particular on the Ice Formation in Polar Seas", (Uber Die Theorie Der Eisbildung, Insbesondere uber Die Eisbildung in Polarmaere) *A. Phys. Chem.*, **42**: 269-286 (1891).

[2] Goodrich L.E., Efficient Numerical Technique for one Dimensional Thermal Problems with Phase Change, *Journal of Heat Mass Transfer*, **21**: 615-621 (1978).

[3] Sparrow J., Ramsey W., Harris S., The Transition from Natural Convection Controlled Freezing to Conduction Controlled Freezing, *Journal of Heat Transfer*, **103**: 7-13 (1983).

[4] Lacroix M., Computation of Heat Transfer During Melting of a Pure Substance from an Isothermal Wall, *Numer. Heat Transfer B.*, **15**: 191-210 (1989).

[5] Yeoh G.H., Behnia M., De Vahl Davis G., Leonardi E., A Numerical Study of Three-Dimensional Natural Convection During Freezing of Water, *International Journal of Numerical Mechanical Engineering*, **30**: 899-914 (1990).

[6] Hadji L., Schell M., Interfacial Pattern Formation in the Presence of Solidification and Thermal Convection, *Physical Review A*, **41**: 863-873 (1990).

[7] Hanumanth G.S., Solidification in the Presence of Natural Convection, *International Communications in Heat and Mass Transfer*, **17**: 283-292 (1990).

[8] Curtic M., Oldenburg F., Spera J., Hybrid Model for Solidification and Convection, *Numerical Heat Transfer, Part B*, **21**: 217-229 (1992).

[9] Trapaga, G., Matthys, E.F., Valecia, J.J., Szekely J., Fluid Flow, Heat transfer and Solidification of Molten Metal Droplets Impinging on Substrates: Comparison of Numerical and Experimental Results, *Metallurgical Transactions B*, **23**: 701-718 (1992).

[10] Watanabe T.I., Kuribayashi Honda T., Kanzawa A., Deformation and Solidification of a Droplet on a Cold Substrate, *Chemical Engineering Science*, **47**: 3059-3065 (1992).

[11] Marchi C., San Liu H., Lavernia E.J., Rangel R.H., Numerical Analysis of the Deformation and Solidification of a Single Droplet Impinging on to a Flat Substrate, *Journal of Materials Science*, **28**: 3313-3321 (1993).

[12] Weidman P.D., Mahalingam S., Axisymmetric Stagnation-Point Flow Impinging on a Transversely Oscillating Plate with Suction, *Journal of. Engineering Mathematics*, **31**: 305-318 (1997).

[13] Shokrgozar Abbasi A., Rahimi,A.B., Non-Axisymmetric Three-Dimensional Stagnation Flow and Heat Transfer on a Flat Plate, *Trans. ASME Journal of Fluids Engineering*, **131(7)**: 074501.1–074501.5 (2009).

[14] Shokrgozar Abbasi A., Rahimi A.B., Three-Dimensional Stagnation Flow and Heat Transfer on a Flat Plate with Transpiration, *Journal of Thermophysics and Heat Transfer*, **23(3)**: 513-521 (2009).

[15] Shokrgozar Abbasi A., Rahimi A.B., Niazmand H., Exact Solution of Three-Dimensional Unsteady Stagnation Flow on a Heated Plate, *Journal of Thermophysics and Heat Transfer*, **25(1)**: 55-58 (2011).

[16] Shokrgozar Abbasi A., Rahimi A. B., Investigation of two-Dimensional Unsteady Stagnation Flow and Heat Transfer Impinging on an Accelerated Flat Plate, *Journal of Heat Transfer*, **134(6)**: 064501-5 (2012).

[17] Shokrgozar Abbasi A., Rahimi A.B. Mozayyeni H., Investigation of Three-Dimensional Axisymmetric Unsteady Stagnation-Point Flow and Heat Transfer Impinging on an Accelerated Flat Plate, *Journal of Applied Fluid Mechanics*, **9(1)**: 451-461 (2016).

[18] Brattkus k., Davis S. H., Flow Induced Morphological Instabilities: Stagnation-Point Flows, *Journal of Crystal Growth*, **89**: 423-427 (1988).

[19] Rangel R., H. Bian X., The Inviscid Stagnation-Flow Solidification Problem, *International Journal of Heat and Mass Transfer*, **39(8)**: 1591-1602 (1994).

[20] Bian X., Rangel R.H., The Viscous Stagnation-Flow Solidification Problem, *International Journal of Heat Mass Transfer*, **39(17)**: 3581-3594 (1996).

[21] Shokrgozar Abbasi A., Rahimi A.B., Solidification of Two-Dimensional Viscous, Incompressible Stagnation Flow, International Journal of Heat Transfer, **135**: 072301-8 (2013).

[22] Shokrgozar Abbasi A., Three-Dimensional Axisymmetric Solidification of a Viscous Incompressible Flow in the Stagnation Point Region, Journal of Applied Fluid Mechanics, **10(1)**: 413-420 (2017).

[23] Gao, J., Lai, Y., Zhang, M., Feng Z., Experimental Study on the Water-Heat-Vapor Behavior in a Freezing Coarse-Grained Soil, *Applied Thermal Engineering*, **128**: 956-965 (2018).

[24] Zhang Y., Zhao W., Ma W., Wang H., Wen A., Li P., Effect of Different Freezing Modes on the Water-Heat-Vapor Behavior in Unsaturated Coarse-Grained Filling Exposed to Freezing and Thawing, *Cold Regions Science and Technology*, **174**: 103038 (2020).

[25] Zheng C., Šimůnek J., Zhao Y., Lu Y., Liu X., Shi C, ... , Su Z., Development of the Hydrus-1D Freezing Module and its Application in Simulating the Coupled Movement of Water, Vapor, and Heat, Journal of Hydrology, 598, 126250 (2021).

[26] Liu F., Jiao X., Wang S., Zhong L. An P., Heat, Water and Vapor Coupled Migration in Loess Under Uniaxial Freezing Condition, *Cold Regions Science and Technology*, **198**: 103550 (2022).

[27] Shokrgozar Abbasi A., Ghayeni M., Vapor solidification of Saturated Air in Two-Dimensional Stagnation Flow, Scientia Iranica, **27(2)**: 693-703 (2020).

[28] Zahmatkesh R., Mohammadiun H., Mohammadiun M., DibaeiBonab M.H., .Sadi.M, Theoretical Investigation of Entropy Generation in Nanofluid's Axisymmetric Stagnation Flow over a Cylinder with Constant Wall Temperature and Uniform Surface Suction-Blowing, *Iranian Journal of Chemistry and Chemical Engineering (IJCCE)*, **40(6)**: 1893-1908 (2021).

[29] Montazeri M., Mohammadiun H., Mohammadiun M., Dibaeebonab M.H., Inverse Estimation of Time-Dependent Heat flux in Stagnation Region of Annular Jet on a Cylinder Using Levenberg-Marquardt Method, *Iranian Journal of Chemistry and Chemical Engineering (IJCCE)*, **41(3)**: 971-988 (2022).

[30] Mohammadiun M., Mohammadiun H., Montazeri M., Momeni A., Dibaeebonab M. H.,Vahidifar S., Mihani S., Naeimabadi M., Sabbaghzadeh F., Inverse Estimation of the Wall Temperature in Stagnation Region of Impinging Flow on the Cylinder with Uniform Transpiration, *Iranian Journal of Chemistry and Chemical Engineering (IJCCE)*, (2023).